Excitation Energy Transfer in Model Light-Harvesting Antennae

Vijaya Subramanian and Deborah G. Evans*

Department of Chemistry, University of New Mexico, Albuquerque, New Mexico 87113

Received: January 23, 2003; In Final Form: July 21, 2003

Applications of light-harvesting arrays range from alternative sources of energy to the field of photonic and optoelectronic devices. Antenna arrays can absorb and transfer light energy to do electrochemical work. Photosynthetic light-harvesting units that are found in nature exhibit highly efficient utilization of solar energy. Recently, biomimetic arrays have successfully been designed. Several questions pertaining to light harvesting arrays still need to be addressed and studied fully. For example, do various antenna geometries give rise to radically different excitation energy transfer, and are the structures in nature especially well-suited for energy transfer? If not, how should specific monomeric structures be arranged to optimize light harvesting? This paper simulates the energy transfer dynamics in several model systems based on monomeric units of the photosynthetic light-harvesting complex, LH2, of purple bacteria using the Haken−Strobl parametrization of the Stochastic Liouville equation. It is found that the coherence size is strongly dependent on the magnitude of the stochastic bath fluctuations and the model geometry. Although static disorder is found to alter the coherence sizes, the overall trends observed in models of increasing ring size do not depend on its absence. A comparison of linear and circular arrays shows that the exciton dynamics has very different scaling properties as a function of array size for the periodic boundary conditions found in ring antenna systems. By monitoring coherence sizes, it is shown that model systems of heterodimers, monomers and homodimers in ring structures exhibit similar energy transfer characteristics. It is also shown that the short-time excitation energy dynamics in coupled ring systems depends on the initial excitation process.

I. Introduction

The conversion of energy from sunlight to usable forms has become enormously important with the increased depletion of traditional fossil fuels. Effective mechanisms for this conversion have been studied for light-harvesting antenna systems that absorb radiant energy that is subsequently converted to electrochemical energy. In addition, applications of light-harvesting antennae as molecular scale devices have also been successful.[1] Synthetic antenna systems consisting of aggregates of molecules that may be connected covalently have recently been synthesized and studied.[2] The structure and chemistry of many artificial systems is modeled very closely on light-harvesting systems found in nature using arrays of porphyrin-based analogues.[1] Reconstitution of light-harvesting systems found in bacteria have also produced biomimetic hybrid biological−chemical structures that contain units held together by a protein environment.[3] These aggregates mimic the behavior of the antenna systems found in nature and allow for synthetic modifications to be made. Suitable artificial light-harvesting arrays should be able to efficiently funnel light energy to a sink where the energy can be stored or converted into useful work. The design of light-harvesting arrays is therefore an important problem and a lot of current work is focused on examining the behavior of these antenna systems as a function of their chemistry and structure.

Light harvesting occurs with very high efficiency in plants and even lower order bacteria. The purple bacteria *Rhodopseudomonas (Rps.) acidophila, Rhodobacter (Rb.) sphaeroides,* and *Rhodospirillum molischianum* represent such systems. The first step in harvesting solar energy is absorption of light by the light-harvesting complexes (LHC). Energy is then funneled to the reaction center (RC) where it initiates an electron-transfer reaction. There are two types of LHCs, the peripheral light-harvesting complex-2 (LH2) and the core light-harvesting complex-1 (LH1). The LH2 complexes absorb sunlight and transfer the excitation energy to the LH1 which in turn transfers it to the reaction center.[4] These light harvesting complexes are membrane bound and embedded in a lipid medium. The LHCs have been isolated and the crystal structure of the LHC in *Rps. acidophila* strain 10050 was determined by McDermott et al. in 1996, followed by the crystal structure of *Rhodospirillum molischianum* by Koepke et al.[5,6] The light harvesting complexes in both cases exhibit circular symmetry. The absorbing bacteriochlorophyll-a (BCHL-a) chromophores that constitute the LH2 in *Rps. acidophila* are held together by a protein scaffold. Twenty seven BCHLs are arranged in two rings, the inner tightly packed ring of 18 BCHLs absorbing at 850 nm (B850) positioned perpendicular to the membrane plane and the 9 outer loosely packed BCHLs absorbing at 800 nm (B800) positioned parallel to the membrane plane (Figure 1). The B850 ring consists of 9 pairs of dimers. The average distance within the B850 dimers is 9.16 and 9.44 Å between dimers. The average distance between the B800's is 18.6 Å, and the chromophores are not dimeric but equidistant from each other. The B800−B850 inter-chromophore distance is also around 18.3 Å. The nine carotenoids absorbing at 500 nm are arranged as shown in Figure 1. The LH2 complex has 9-fold symmetry with 2 B850s, 1 B800, and 1 carotenoid in each symmetric subunit.

The determination of these crystal structures has prompted intense research by providing inter-chromophore distances from which coupling strengths and site energies can be determined using a variety of approximations and ab initio electronic structure methods.[7] The presence of chromophores absorbing

* To whom correspondence should be addressed. E-mail: debi@unm.edu.

10.1021/jp034196b CCC: $27.50
Published on Web 12/24/2003

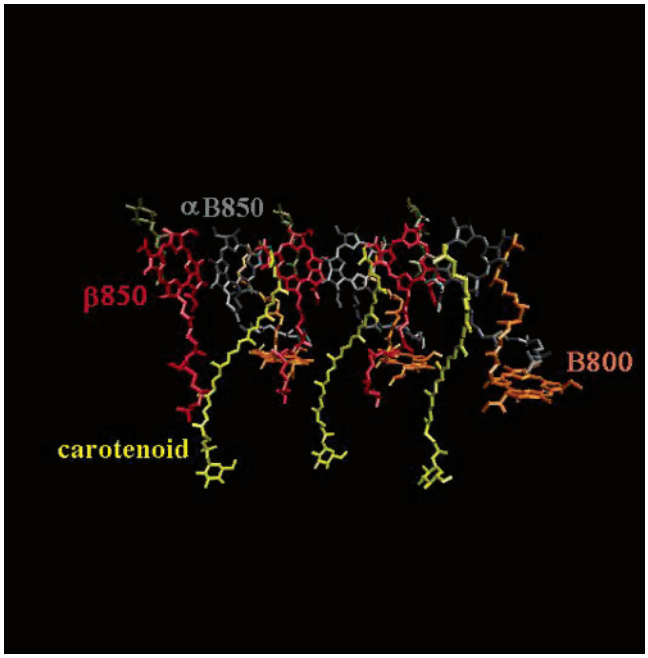

Figure 1. Chromophores in the two rings of the LH2 of *Rps. acidophila*. The αB850 (red), *β*B850 (grey), B800 (orange), and carotenoid (yellow) molecules are highlighted. Only a third of the ring is displayed and the protein scaffold is not shown for clarity.

at different frequencies enables absorption in a wide region of the solar spectrum, and it is believed to enhance the light harvesting capabilities of the bacteria.[4] Energy absorbed by the higher energy chromophores, the B800 BCHLs and the carotenoids, is thought to cascade into the B850s before being transferred to the LH1 subunit and the photosynthetic reaction center.[4] The transfer times between the LHCs is crucial in ensuring the greater than 95% efficiency observed in nature as the entire process has to occur before fluorescence leads to energy loss.[4]

Various reasons have been given for the circular symmetry of the LHCs in nature. One of the possible explanations is the equivalence of the chromophores in the circular geometry which would lead to more efficient transfer between complexes. The other possible reason put forward by Schulten and co-workers is that the lowest excitonic state in the B850 ring is a dark state, and thus, the transition from the doubly degenerate bright states to the dark state after the absorption step would reduce fluorescence emission considerably.[8] Subsequent studies by Damjanovic and co-workers have shown that disorder leads to an intensity distribution over a number of eigenstates;[9] thus, the above explanation does not fully account for the presence of the circular geometry in LHCs. Ritz and co-workers[11] have also studied the transfer of excitation energy between the antenna complexes and subsequent transfer to the RC using two specific arrangements of the complexes in the membrane, and their calculations yield good estimates for the overall efficiency of light harvesting, but the importance of circular rings in determining the high efficiency as compared to other geometries of the individual LHCs is not clear. The presence of two concentric rings in the B850−B800 composite system within the LHC-II expands the range of the solar spectrum that can be harvested. It has been postulated that the dimeric structure of the B850 ring leads to the formation of two excitonic bands with the higher band lying close to the B800 band leading to more efficient transfer of energy between the rings.[10] Experimental work has also been carried out by Herek et al.[12] in a study of the composite B800−B850 system. A series of reconstituted LH2 complexes from *Rps. acidophila* with a progressive blue-shift in the peak maximum of the B800 band was studied for its effect on energy transfer. Blue-shifting the peak maximum resulted in a pronounced decrease in energy transfer rates. This effect has also been observed when the B850 peak maximum was blue-shifted toward the B800 peak maximum in a series of mutants which lead to an increase in transfer rates.[13]

Excitation energy transfer within the LH1 and LH2 complexes following absorption of solar energy has been studied extensively by both experimental and theoretical methods. Modeling ultrafast fluorescence up-conversion experiments using the dimer hopping model, Jimenez et al. estimated the transfer time within the B850 ring to be around 100 fs.[14] Using a variety of techniques, including the three pulse photon echo peak shift experiments, the B800−B850 and the B800−B800 transfer times have been estimated to be around 650−800 and 500 fs−1 ps, respectively.[15,16] The inter-complex transfer times are in the picosecond range with the LH2-LH1 transfer time around 3 ps at room temperature.[4b] The rate-limiting step in the light harvesting process is the transfer of the excitation from LH1 to the reaction center, which is estimated to be ≈35 ps.[4b]

One of the issues studied previously is whether the excitation energy transfer is coherent or incoherent. Both dynamic and static disorder affect energy transfer in the antenna complexes and may lead to exciton localization and incoherent transfer.[4] The transfer rates within the rings and between rings depends on whether the energy transfer is coherent or incoherent. There is experimental evidence for some degree of coherence in the B850 ring: the circular dichroism spectrum shows a strong peak near the lower absorption band of the B850 ring that can be fitted with a model where the exciton is delocalized over almost the entire ring.[7d] Detailed modeling of the CD spectra by van Grondelle et al. required at least a large part of the complete ring.[17,18a] In a more recent paper, these authors obtain a much smaller value of 3 pigments[18b] using a different measure of exciton localization. Monte Carlo simulations of superradiance data indicate that the exciton delocalization length is about 3−4 pigments at room temperature.[19] Absorption difference spectra of two-color excitation experiments have been modeled, using different aggregate sizes within the ring, to yield a coherence length of 4 ± 2 chromophores.[20] Transient absorption spectra have also been simulated, including the effects of static diagonal disorder, and a delocalization length of 4 ± 1 chromophores was determined.[21] A comparison of the various measures of coherence used in the energy transfer literature is discussed in the paper by Dahlbom et al.[22] The discrepancies in the actual magnitude of the coherence size reported in the literature can be attributed to the different measures used to calculate or determine this property.

Theoretical studies have used path integral methods, time-dependent density matrix methods, and relaxation approaches to understand various aspects of light harvesting. Studies by Ray and Makri and Damjanovic et al. indicate that the room temperature localization of the exciton is largely due to averaging over a Boltzman distribution of excitonic states and much less dependent on dynamic localization.[23] Recently, some single molecule spectroscopic data have been interpreted in terms of completely delocalized excitonic states,[24] although theoretical studies have contested that idea.[17] Density matrix methods such as the Redfield approximation[25] have been used to study the temporal evolution of the excitons after B800 excitation.[26a] B800−B850 transfer times have been estimated and observed to match experimental values when the upper band

edge of the B850 ring was adjusted to be close to the B800 band center. In a subsequent Redfield study,[26b] exciton dynamics in the B850 system was studied including the effect of static diagonal disorder. These studies showed that both static and dynamic disorder are important in the LH2 array and that the coherence size is affected by dynamic disorder. At short time delays, the exciton coherence domain was found to extend over the entire ring and asymptote to about four sites.

Recent studies of artificial antenna systems have shown that synthetic mimics of the light-harvesting systems found in nature can be made. Many of the most successful mimics have used porphyrin derivatives as the building blocks of functioning arrays. In addition successful synthetic analogues that incorporate a "reaction center" unit have been achieved using fullerene derivatives.[2a] Reconstituted biological systems have been synthesized from LH2 as hybrid chemical−biological mimics.[3] Another class of branched macromolecules, called dendrimers, have also been studied quite extensively as energy-funneling devices.[2b] The excitation of species on the periphery of the dendrimer has been followed by excitation energy transfer toward the center of the structure if a sink is placed at the core. Studies have shown that the efficiency of this funneling depends sensitively on the branching of these structures and the overall topology differences between condensed and extended dendrimers.[27] To date, the efficiency of artificial systems does not approach that of natural systems. In general, the artificial systems do not have extensive arrays that can absorb over a range of the solar spectrum, neither do artificial systems contain such an extensive arrangement of antenna units into larger assemblies. With the ability to control the structure and chemistry of artificial systems, several important questions arise concerning the future design of light-harvesting systems.

Certainly, experimental work has already looked at the effects of the electronic and chemical properties of the monomer units and the connection to optimizing high quantum yields.[2a,28] For systems of a given chemistry, however, it is likely that geometry plays an important part in the energy transfer dynamics. Although the synthetic rearrangement of units in an extensive assembly of light-harvesting units would be extremely time-consuming, simulations of specific model systems can be done efficiently to address issues concerning the structure of efficient light-harvesting systems. Questions pertaining specifically to the arrangement of monomeric units that need to be addressed include (1) How does the geometry affect the energy transfer processes within a given antenna complex? (2) How does the geometry influence energy transfer between antenna complexes in an extensive assembly? The primary goal of this paper is to conduct a study that addresses issues related to the first question: specifically, how does geometry of an antenna system affect the energy transfer dynamics? The comparison of many different geometries is done using models for the monomeric units which are based on the LH2 system found in nature. In this way, the effects of geometry are isolated and examined for porphyrin-based systems. In so doing, the geometries of light-harvesting units found in the highly efficient natural systems can be compared directly with other arrangements. The comparison is achieved by examining the energy transfer dynamics following absorption of energy in different model antenna systems.

In previous studies of molecular aggregates, comparison of the absorption spectra and the participation ratio of linear arrays have been studied as a function of the system size.[29] The monomeric units were not chosen to be specific chemical systems and the array sizes were much larger, 100−250 monomers, than LH2 or any of its mimics. Absorption spectra of uniform circular arrays with fixed radius and varying number of chromophores have also been studied using a Frenkel exciton model and dichotomic white noise for the bath dynamics.[30] In these studies, the absorption spectra are shown to be sensitive to the dipole orientations of the monomers for rings with up to twelve monomers.

In this study, the exciton dynamics is coupled to a dissipative bath that represents the dynamics of the solvent and nuclear vibrations. For the study of a large number of different structures that can be arranged in extensive arrays, the solution of the dynamics is most easily achieved using an efficient computational approach. In this study, we use the stochastic Liouville equation as parametrized by Haken and Strobl[31] to study exciton dynamics in antenna systems of a variety of sizes and geometries. One limitation of the SLE is that it gives the infinite temperature limit at long times. Although this is a disadvantage when studying exciton dynamics at low temperatures, it can give a good qualitative description of the short time dynamics of real systems at finite temperatures. When additional simplifying approximations are made concerning the system-bath coupling, the SLE can be solved using symmetry factorizations that lead to very sparse propagation matrixes which reduces the computational effort considerably. The monomeric building blocks are based on the porphyrin chromophores found in LH2 of the purple bacterium *Rhodopseudomonas acidophila* strain 10050 and *Rhodobacter sphaeroides*. The aim is to compare the energy transfer in ring assemblies of various sizes directly with linear arrangements of the same chromophores, using the same bath parameters and methodology. The effects of the number of subunits, the site energies, and the coupling strengths (i.e., homodimeric, heterodimeric, and monomeric arrangements) in a model of the B850 ring found in LH2 are calculated using the SLE. The effect of the magnitude of the bath fluctuations as well as that of static diagonal disorder on the coherence in the ring is also included. The role of inter-ring transfer is examined by modeling a coupled B850 and B800 ring system, and the effects of initial excitation on the resultant exciton dynamics are simulated. The numerical techniques are discussed in sections II and III. The results for the model systems are given in section IV, and the main observations and conclusions are given in section V.

II. Computational Methods

The coupling strengths between the chromophores relative to the absorption energies requires that a Frenkel exciton model be used to model systems based on LH2. The presence of dimers in the ring of chromophores leads to two excitonic bands.[41] In the model systems studied here, the chain of chromophores is described by the Frenkel exciton Hamiltonian including dynamic disorder

$$H = \sum_n \epsilon_n b_n^\dagger b_n + \sum_{n\neq} \sum_{n'} h_{nn'}^0 b_n^\dagger b_{n'} + \sum_n \sum_{n'} h_{nn'}^1(t) b_n^\dagger b_{n'} \quad (1)$$

where n is the site index, $b_n^\dagger$ and b_n represent exciton creation and annihilation operators respectively, ϵ_n represent site energies, and $h_{nn'}^0$ represents the coupling elements between sites. The last term, $h_{nn'}^1(t)$, represents the stochastic fluctuations of the site energies and couplings due to system−bath interactions. The bath is treated classically with the stochastic fluctuation terms taken to be white noise and parametrized according to Haken-Strobl as follows:

$$\langle h_{n_1 n2}(t)\rangle = 0 \tag{2}$$

$$\langle h_{n_1 n_1'}(t_1) h_{n_2 n_2'}(t_2)\rangle = 2\Lambda(n_1, n_1', n_2, n_2')\delta(t_1 - t_2) \tag{3}$$

with

$$\Lambda(n_1, n_1', n_2, n_2') = \gamma_{n_1 n_1'}\delta_{n_1 n_2'}\delta_{n_1' n_2} + \bar{\gamma}_{n_1 n_1'}\delta_{n_1 n_2}\delta_{n_1' n_2'}(1 - \delta_{n_1 n_1'}) \tag{4}$$

The mean of the fluctuations is assumed to be zero (eq 2) and the fluctuation correlation terms (eq 3) are delta correlated indicating that no memory of past interactions between the system and bath exist at any given time. In addition, correlations between fluctuations in site energies of the different chromophores are set to zero as are the correlations between fluctuations in the coupling elements between different pairs of chromophores (eq 4). These assumptions are strictly valid only when the exciton bandwidth is smaller than kT, but the short time dynamics should reproduce room temperature behavior of exciton migration in light-harvesting systems reasonably accurately.

Within the Haken−Strobl parametrization of the Stochastic Liouville equation the equation of motion for the reduced density matrix, ρ for exciton dynamics is given by

$$\dot{\rho}_{nn'} = -i[H_0,\rho]_{nn'} - \delta_{nn'}\sum_{n_1}(\gamma_{nn_1} + \gamma_{n_1 n})(\rho_{nn} - \rho_{n_1 n_1}) - (1 - \delta_{nn'})(\Gamma\rho_{nn'} - 2\bar{\gamma}_{nn'}\rho_{n'n}) \tag{5}$$

where $\Gamma = \sum n_1 (\gamma_{nn_1} + \gamma_{n_1 n'})$ and n is the site index. The above equation is general and applicable to linear chains as well as rings of chromophores,[32] and it leads to N^2 coupled ordinary differential equations, where N is the number of sites or chromophores in a chain. When translational symmetry and periodic boundary conditions are applied, as in symmetric ring assemblies, the N^2 equations factorize into smaller sets of coupled equations when expressed in terms of the eigenstate basis. The size is reduced by a factor of M, where M is the number of symmetric subunits present. For example, for the 27 chromophore LH2 complex, there is a 9-fold reduction in the size of the coupled sets of equations. In this work, the equations of motion for the reduced density matrix were generated symbolically within Mathematica[33] in the eigenstate basis for each particular model system. The coupled equations were then solved numerically for each parameter set using Gear's method for stiff equations.[34]

The characteristics of exciton migration were studied by following population transfer rates and the temporal evolution of the coherence size. The off-diagonal elements of the exciton density matrix represent coherences or interferences between the different excitonic states and have an impact on transfer rates between them. The inverse participation ratio as defined by Meier and co-workers gives an estimate of the magnitude of the coherences.[35] The coherence size, L_{coh}, is given by the expression

$$L_{\mathrm{coh}} = \frac{(\sum_{nn'}|\rho_{nn'}|)^2}{N\sum_{nn'}|\rho_{nn'}|^2} \tag{6}$$

where N is the number of sites or chromophores. L_{coh} runs between $1/N$ and N. When density is localized on one site, the coherence is $1/N$. When the density matrix is diagonal with all values equal, the magnitude of the coherence is 1. This happens when all excitonic states become equally populated, i.e., in the infinite temperature limit. This definition includes both dephasing and diagonal and off-diagonal matrix elements, and consequently, we have used it as a measure in our comparative studies. The time evolution of the coherence size reflects the dynamics of the density matrix elements. If this density is delocalized over several sites, this affects both intra- and inter-array exciton transfer.

The SLE has been used in many previous studies, including a brief study of exciton dynamics in chains of dimers.[36] However, this description focused on homodimers and parameter regimes where the coupled equations reduce to a master equation description of the system. The SLE has also been used in an early study of excitation energy transfer in photosynthetic units where the effects of quenching and coherent and incoherent transfer on quantum yields were determined.[37] The model studied was a circular aggregate of 24 chromophores with a quenching reaction center in the middle. The conclusion reached in that study was that coupled coherent−incoherent transport leads to a high quantum yield of energy transfer to the reaction center for the above geometry, although as a model for LH2, unrealistically low inter-chromophore coupling strengths of 11−110 cm^{-1} were used.

SLEs have also been used more recently to successfully model exciton dynamics and spectral features of the LH2 system[38] and synthetic energy transfer molecules.[39] Other simulations of the spectroscopy of LH2 have used the Redfield density matrix approximation. The Redfield equations provide a way to study the problem of exciton dynamics coupled with the effects of bath dissipation by incorporating the bath influence into the Redfield tensors. In the most general case, this formalism results in a highly coupled equation of motion for the exciton dynamics that can only be solved to long times using large-scale matrix techniques. For the studies proposed here, the disadvantage of this method is that it is also not possible to use symmetry factorization to reduce the computational effort or simplify interpretation of the results. Master equations obtained from the secular approximation to the Redfield equations also yield simplification of the dynamics. However, because more off-diagonal dephasing terms can be retained in the SLE than in this master equation approach, the SLE has been used here.

III. Model System Parameters

The model systems studied here are based on the purple bacterium *Rps. acidophila* for which the crystal structure is available.[5] The interaction potential between the chromophores can be expressed in terms of the coulomb and exchange interactions. The exchange term decays rapidly with internuclear distance and is appreciable only when there is overlap between the interacting orbitals, whereas the coulomb interaction is long range. Approximate methods are generally used to calculate these interactions. The leading term in the expansion of the coulomb interaction term, the dipole−dipole term is given below

$$V_{\mathrm{dip-dip}} = C[(\hat{n}_i.\hat{n}_j - 3(\hat{n}_i.\hat{r}_{ij})(\hat{n}_j.\hat{r}_{ij})]/r_{ij}^3 \tag{7}$$

where $\hat{n}_i$ and $\hat{n}_j$ are unit vectors pointing in the direction of the transition dipoles associated with chromophores i and j and $\hat{r}_{ij}$ is the unit vector connecting the centers of the two chromophores. The magnesium atom is assumed to be the center of the chromophore. The transition dipoles in the bacteriochlorophylls point from the nitrogen labeled ND to the nitrogen labeled NB in the crystal structure. The magnitude of the constant C, which takes into account the effect of the dielectric constant of

TABLE 1: Nearest-Neighbor (αB850$-\beta$B850)$_1$ and Next-to-Nearest Neighbor (αB850$-\beta$B850)$_2$ Coupling Strengths Used in the Different Ring Types

coupling	monomer[a]	KSF−I[b]	KSF−II[b]	dip−dip[b]	hom[a]
(αB850$-\beta$B850)$_1$ cm^{-1}	225	238	320	385	238
(αB850$-\beta$B850)$_2$ cm^{-1}	225	213	255	270	213

[a] The site energies are all equivalent. [b] The site energies of the αB850=803 nm and the βB850=823 nm.

the medium and the strength of the transition dipoles, was obtained from the paper by Jang et al.[40]

The coupling strengths between the chromophores in the model systems studied were calculated using the dipole−dipole approximation. The dipole−dipole approximation is often used in describing the interaction between the chromophores though it is known to overestimate the coupling strengths. However, it might reasonably be expected that the dipole−dipole approximation is sufficient for studying general trends in exciton transfer in the model systems studied here. To check this, the dynamics in the 18 membered B850 ring system was compared using the coupling strengths determined by Kroeger, Scholes, and Fleming (KSF) using the transition density cube method[7a] where only the coulomb interaction is considered (KSF−I) and coupling strengths where both coulomb and exchange interactions were considered (KSF−II).[7b] The site energies of 803 and 823 cm^{-1} used for the α-B850 and the β-B850 chromophores respectively were taken from previous studies of the bacterium *Rhodobacter sphaeroides* which is found to have very similar light harvesting characteristics to *Rps. acidophila*.[41]

IV. Results and Discussion

IV.A. In this section, the effect of varying the ring type and coupling strengths on excitation energy transfer within an 18-membered B850 ring assembly is studied. Calculations on excitation energy transfer have been carried out by various authors by considering different coupling strengths between the chromophores within the 18-membered B850 ring of LH2 based on the structural parameters obtained from the crystal structures and the different levels of theory used.[7b,d,20] Experimentally determined coupling strengths are of the same order of magnitude as the theoretically estimated values, but there is a maximum variation of about 160 cm^{-1} in the coupling strengths which could possibly have an impact on exciton dynamics. In addition, the dynamics and stationary spectra are often modeled using identical site energies for the α and β B850 chromophores essentially making the system homodimeric.

Recent work has shown that optimal control of energy transfer in LH2 is possible using adaptive shaping of laser pulses.[42] As we also show below in section IV.C, the initial excitation plays an important role in determining energy transfer rates. Because different structures would be expected to have different optimal excitation profiles, the relatively straightforward choice of localized initial excitation is made here only to simplify the comparison between many structures and demonstrate exciton dynamics following an excitation. To estimate the effect of all of the variations in ring type and coupling strengths, we have studied the following systems using the SLE:

(1) An 18 chromophore ring with the chromophores arranged as a chain of monomers. All of the site energies are equal, and the coupling strengths between the chromophores are set to values that are an average of the two largest couplings found in the heterodimer with KSF−I parameters (Table 1). (2) An 18 chromophore ring with the chromophores arranged as a chain of dimers with equivalent site energies (homodimer). The coupling strengths are set to the same values as the heterodimer with KSF−I parameters. (3) An 18 chromophore B850 ring with the chromophores arranged as a chain of dimers with inequivalent site energies (heterodimer). The parameters chosen are KSF−I. (4) An 18 chromophore ring with the chromophores arranged as a chain of dimers with inequivalent site energies (heterodimer) but with the coupling strengths determined using the dipole−dipole approximation. (5) An 18 chromophore ring with the chromophores arranged as a chain of dimers with inequivalent site energies (heterodimer). The parameters chosen are KSF−II.

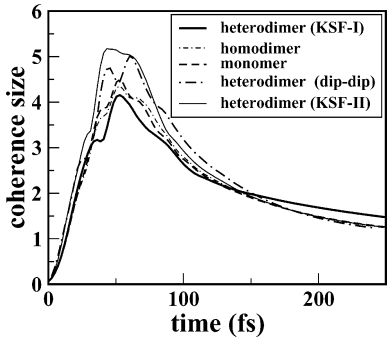

Figure 2. Comparison of exciton dynamics in different ring types. The coherence size changes by one unit with a change of ≈147 cm^{-1} in the magnitude of the coupling constant from the (KSF−I)-heterodimer to the (dip-dip)-heterodimer. Dimerization does not lead to significant changes in the coherence size.

Although the couplings between all of the chromophores were used in the calculations, only the largest are presented in Table 1 as the longer range couplings are insensitive to the method used in estimating them.[7a,40] The on-site relaxation constants ($\hbar\gamma_{nn}$) were set to 110 cm^{-1} and the off-diagonal nearest-neighbor (αB850$-\beta$B850)$_1$ and next-to-nearest neighbor (αB850$-\beta$B850)$_2$ fluctuation constants were fixed at 2.37 and 2.19 cm^{-1}, respectively, in all cases. All other fluctuation constants were set to zero. The strong coupling between the B850 chromophores leads to a rapid rise in coherence size on the order of tens of femtoseconds with the coherence peaking around 100 fs in all cases as seen in Figure 2. We find that the effect of the variations in ring type to be minimal with a difference of about 1 unit in coherence size for a maximum difference of 147 cm^{-1} in coupling strengths between the chromophores. As the exciton transfer dynamics within the B850 ring is found to be fairly insensitive to the coupling strengths within reasonable bounds, the dipole−dipole interaction parameters were used in all other model B850 systems studied. Although the coherence size of a larger ring is unaltered by small modifications in the arrangement of the monomers, the design of light-harvesting antenna arrays based on systems found in nature could, in principle, be optimized in a variety of ways. For example, the ring size and the number of monomers can be altered, and arrays with other shapes can be constructed. To examine if the ring geometries generally found in nature display different excitation dynamics, other arrays are studied in sections IV.B and IV. C.

In the SLE, the role of the bath is stochastic. The effect of varying the relaxation constants on exciton dynamics in a B850 ring with 18 chromophores arranged in dimeric pairs is studied using the parameters given in Table 1 (heterodimer, KSF−I). The on-site fluctuations are found to be about 2 orders of magnitude larger than the off-diagonal fluctuations in certain crystalline systems.[31b] Damjanovic et al.[9] determined from their molecular dynamics simulations that the diagonal fluctuations

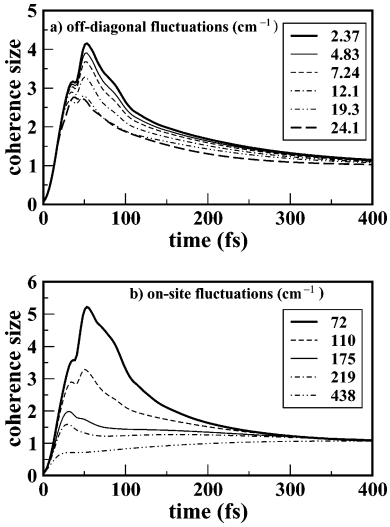

Figure 3. (a) On-site relaxation constant which was set at a constant value of 110 cm^{-1}. The off-diagonal relaxation constants were varied from 2.37 to 24.1 cm^{-1}. (b) The effect of the on-site relaxation constants was monitored at a constant value of the off-diagonal relaxation constant.

TABLE 2: Off-Diagonal Nearest-Neighbor (αB850−βB850)$_1$ and Next-to-Nearest Neighbor (αB850−βB850)$_2$ Fluctuations Corresponding to Figure 3A[a]

(αB850−βB850)$_1$ $\hbar\gamma$ cm^{-1}	(αB850−βB850)$_2$ $\hbar\gamma$ cm^{-1}
2.37	2.19
4.83	4.39
7.24	6.58
12.1	11.0
19.3	17.6
24.1	21.9

[a] All other fluctuation constants were set to zero. The on-site fluctuation constant was fixed at 110 cm^{-1}.

are 2 orders of magnitude larger than the off-diagonal fluctuations in the LH2 of *Rs. molischianum*. We have varied the fluctuations around what the homogeneous line-width is estimated to be for the LH2 of photosynthetic bacteria from fits to experimental data. Homogeneous line widths determined from fits to absorption difference spectra recorded at 300 K are found to be around 75 cm^{-1}.[21] Simulation of three-pulse photon echo experiments on the other hand yielded a homogeneous line width of 188 cm^{-1}.[43] In contrast with other studies on LH2,[26b] in this section, we varied both the diagonal and off-diagonal fluctuations independently in order to examine the role of each. In Figure 3a, the on-site fluctuation is set at 110 cm^{-1} and the nearest-neighbor (αB850-βB850)$_1$ off-diagonal fluctuations are varied from 2.37 to 24.1 cm^{-1} (Table 2). The exciton dynamics is studied by looking at the coherence size as a function of time. We find that the coherence size depends very strongly on the off-diagonal fluctuations even though the magnitude of the fluctuations is quite small. As expected, the coherence size decreases as the system bath coupling terms become larger. Our studies of off-diagonal dynamic disorder show that the system is extremely sensitive to small changes in their magnitude. In Figure 3b, the off-diagonal nearest-neighbor (αB850−βB850)$_1$ and next-to-nearest neighbor (αB850−βB850)$_2$ fluctuation constants were fixed at 12.1 and 11.0 cm^{-1}, respectively, and the on-site fluctuations varied through a wide range of values. Here the impact of bath relaxation constants is even higher. The coherence size drops to its minimum value as the magnitude of the on-site fluctuations is increased. The exciton dynamics is extremely sensitive to the strength of these bath fluctuations.

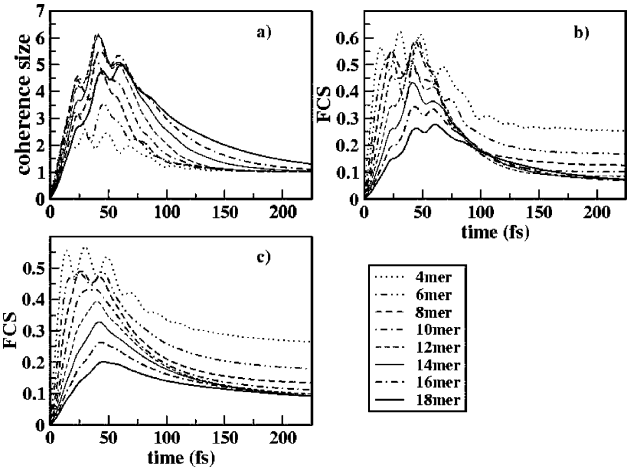

Figure 4. Exciton dynamics in rings of different sizes. In (a), the coherence size increases with ring size, maximizing at the 12mer. In (b), the fractional coherence size (FCS) is plotted as a function of time. In (c), the FCS is plotted for the same parameters as in (b) but with the inclusion of static disorder.

In previous work, experimentally observed population transfer rates in the B800−B850 system following excitation at 800 nm have been modeled using the Redfield approximation with different parameter sets for a stochastic bath.[26a] The experimental data was best modeled using diagonal relaxation parameters of 100 cm^{-1} for the B850 chromophores and setting the off-diagonal fluctuations to zero. The dynamics was found to be sensitive to the bath relaxation constants within the three parameter sets that were used in the study. The sensitivity varied depending on the parameters used for the site energies of the chromophores as well as the coupling strengths used. In another Redfield study,[26b] exciton coherences were calculated by varying the static disorder, the magnitude of the bath-induced relaxation, and setting the bath parameters to values optimized by modeling experimental data. These studies showed that both static and dynamic disorder are important in the LH2 array and that the coherence size is affected by dynamic disorder. It is important to note that the results presented here using the parametrized stochastic Liouville equation yield similar coherence size dynamics to the above-mentioned Redfield simulations. The SLE dynamics therefore captures the right trends found in LH2 and this validates the parameters chosen here to simulate energy transfer in general porphyrin-based arrays. The effect of static disorder is investigated in the next section.

IV.B. This section addresses the effects of ring size on exciton dynamics. To determine whether the 18-membered ring in LH2 has any special properties, rings of different sizes were generated by rotating one dimeric subunit of the 18 membered LH2 of *Rps. acidophila* through ($2\pi/N$), with N ranging from 2 to 9. The distance between the dimers is kept at the constant value of 9.16 Å observed in LH2 of *Rps. acidophila*. This results in rings of varying radii and number of chromophores but fixed nearest-neighbor interactions. The exciton dynamics is monitored by plotting the coherence size as a function of time. The on-site relaxation constants ($\hbar\gamma_{nn}$) were set to 110 cm^{-1} and the off-diagonal nearest-neighbor (αB850−βB850)$_1$ and next-to-nearest neighbor (αB850−βB850)$_2$ fluctuation constants were fixed at 2.37 and 2.19 cm^{-1}, respectively, in all cases. All other fluctuation constants were set to zero. A fairly dramatic change is observed on going from the ring with two dimers (4mer) to the ring with 6 dimers (12mer) as seen in Figure 4a. The coherence size then levels off beyond the 12mer with a small dip at 9 dimers (18mer). A plot of the fractional coherence size

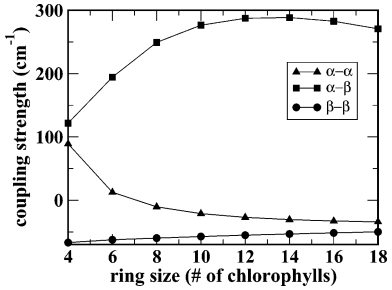

Figure 5. Variation in the next-to-nearest neighbor couplings plotted as a function of the ring size. The $\alpha-\beta$ coupling increases rapidly on going from the 4mer to the 10mer and the levels off with increasing ring size. The $\alpha-\alpha$ coupling constant decreases with increasing ring size and then saturates at the 10mer. The $\beta-\beta$ coupling constants are fairly constant.

(FCS), i.e., the coherence size divided by the number of chromophores in the ring, in Figure 4b shows that the FCS is relatively constant in the three smallest rings and then starts dropping as the ring size increases. The change in coherence size as a function of the ring size can be explained quite simply by looking at the variation in the next-to-nearest neighbor couplings as a function of ring size. As seen in Figure 5, the next to nearest neighbor couplings between the α and β chromophores varies rapidly on going from the 4mer to the 12mer and then saturates with a slight dip at the 18mer. Similarly, the $\alpha-\alpha$ next-to-nearest neighbor couplings change rapidly when going from the 4mer to the 12mer and saturates for the higher ring sizes. The $\beta-\beta$ couplings change minimally. The change in coherence size as the ring size changes mirrors the changes in the couplings very closely. The fractional coherence size on the other hand appears to saturate for the smaller rings and decreases as the ring size increases. This is due to the fact that the coupling strength changes are compensated for by the change in ring size for the smaller rings thus giving rise to a constant fractional coherence size, but this is no longer true for the larger rings so the coherence size decreases.

The role of static disorder in LH2 has been examined in previous work on photosynthetic antenna systems.[9,22,26a,b,40] Static disorder reduces the coherence size but the signature of coherent energy transfer in these systems is clearly apparent. The paper by Jang et al. which looks exclusively at static disorder shows that both diagonal and off diagonal disorder likely contribute to the observed energy transfer behavior in antenna systems. Static off-diagonal disorder is not considered in the paper by Dahlbom et al.,[22] but the study takes into account the effect both static and dynamic disorder on coherence size and energy transfer. For the model systems studied in this paper, the focus is on comparing the behavior of different model geometries for which exact values of static and dynamic disorder are not known. We have consequently used a value of 255 cm^{-1} for the width of the Gaussian static diagonal disorder as given in the paper by Dahlbom et al.[22] The parameters chosen for the dynamic disorder are the same as in Figure 4, parts a and b. The propagations were carried out using a fourth order Runge−Kutta algorithm. Averaging over 2500 realizations, the FCS for the various rings is as shown in Figure 4c. The pattern of the saturation behavior is very similar in Figure 4, parts b and c. Obviously in Figure 4c, with the presence of additional static disorder, the coherence sizes are smaller by about 1 unit. However, note that the coherence size saturates with increasing ring size even in the presence of static disorder of the magnitude found in LH2.

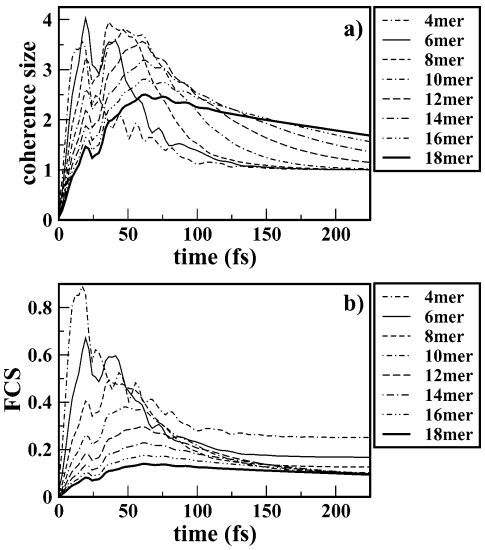

Figure 6. (a) Coherence size and (b) FCS plotted for linear chains. The relaxation constants are the same as that for the ring systems in Figure 4. The largest next-to-nearest neighbor coupling is constant at 422 cm^{-1}. There is no saturation in coherence size with increasing chain length. The FCS decreases monotonically with increasing chain length.

The most interesting and important finding here is that the coherence size saturates for the larger rings. This behavior is directly related to the circular boundary conditions. Energy transfer between arrays depends on the coherence size. Delocalization over several sites can enhance excitation transfer to another array if the arrays are suitably arranged relative to each other. In addition, if the ring arrays are larger, more efficient excitation transfer can occur between them. The cyclic properties of ring arrays result in larger coherence sizes for relatively large assemblies. In nature, several light-harvesting complexes have ring structures, and typically, these ring arrays are about the same size as the saturation limit of 12−18 monomers found here. Synthetic light harvesting arrays have been synthesized in a variety of geometrical arrangements. Consequently, an important question that has not been addressed previously is how does the behavior of ring assemblies depend on the geometric arrangement of monomers in an array. In this work, we study two different geometric arrangements of monomers: linear and ring arrays. Excitation energy transfer in linear arrays of different sizes is compared with that in ring systems using the same monomeric units, initial excitation, and dissipative bath.

The basic dimeric unit found in the 18 membered B850 ring of *Rps. acidophila* was extended in one dimension while maintaining the inter-dimer distance constant at the value observed in the ring. The change in geometry results in a higher inter-dimer coupling constant (422 cm^{-1}) than that found in the ring structure. The exciton dynamics in these linear chains with the same set of relaxation parameters as used for the model rings is shown in Figure 6, parts a and b. The coherence size decreases with increasing chain length and has a value of $\approx$2.4 for the 18 membered chain. The coherence size is found to be less than that for the corresponding rings except in the case of the 4mer. The difference in coherence size between the linear chains and rings increases with the number of dimers present. Because there is no saturation of the coherence length, a monotonic decrease in fractional coherence size is observed in the linear chains. It might be suspected that this striking contrast in behavior is due simply to the change in the exciton coupling parameters due to the change in geometry. This was checked by looking at excitation energy transfer in linear chains of

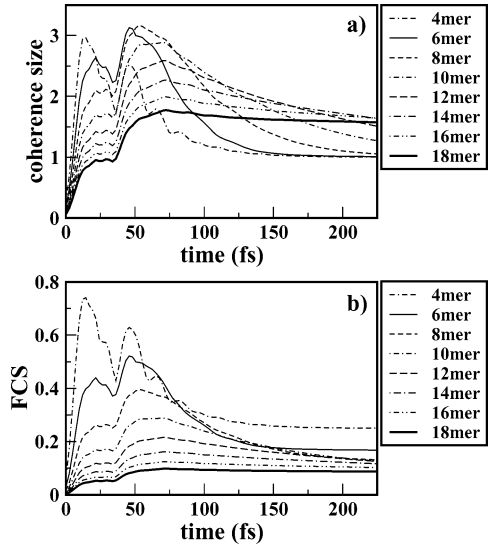

Figure 7. (a) Coherence size and (b) FCS plotted for linear chains with the largest next-to-nearest neighbor coupling set to the value found in the 18 membered B850 model ring. The relaxation constants are set to the same values used in the model ring systems.

various sizes with the inter-dimer coupling constant set to the value of 271 cm^{-1} found in the 18-membered ring (Figure 7, parts a and b). Apart from a decrease in the absolute value of the coherence size in all of the chains compared to Figure 6a, the pattern of the variation of coherence size as a function of chain length remains unchanged. It is therefore clear that dynamic disorder has a much greater effect on exciton localization in linear assemblies of dimers as the chain size increases than in the corresponding ring structures. This can be attributed to the lowering of symmetry and the loss of periodicity on going from the ring structure to the linear chain. The symmetry of the ring structures leads to enhanced coherences and also acts as a buffer against the effects of dynamic disorder. From this study, and the parameter set used herein, it is found that enhanced control over excitation energy transfer favors ring geometries in the design of light harvesting antenna, though linear chains may be simpler to synthesize.

IV.C. As noted in section IV.A, actual light-harvesting assemblies, like the LH2 found in nature in Figure 1, are composed of many arrays that transfer energy from one to another to a sink where the energy is converted to useful work. In LH2, each B850 ring is associated with a ring of B800 chromophores. Most experiments on the B850 system have been carried out by first irradiating the B800 chromophores and following exciton dynamics after downhill energy transfer to the B850 chromophores. The delocalization lengths have been determined from the transient absorption spectra obtained. The possibility that the delocalization length would be different depending on which chromophore is initially excited has been alluded to by Chachisvilis et al. and Pullerits et al. but no numerical simulations or experimental studies have been carried out to check the validity of the assumption.[20,21] Jimenez et al. have carried out an experimental study of excitation energy transfer by direct excitation of the B850 chromophores as well as after exciting the B800 chromophores. Although no measurements related to the dynamic coherence size or delocalization length within the B850 ring were made for the two modes of excitation, the B800−B800 excitation energy transfer rates were determined from anisotropy data.

The effect of a B800 ring on the excitation transfer dynamics in the B850 ring is important for understanding light-harvesting

TABLE 3: Nearest-Neighbor and Next-to-Nearest Neighbor Coupling Strengths Used in the B800−B850 Composite System[a]

coupling	coupling strength (cm^{-1})
$(\alpha B850-\beta B850)_1$	238
$(\alpha B850-\beta B850)_2$	213
B800−αB850	27
B800−βB850	23
B800−B800	−26

[a] The site energies of the αB850 = 803 nm, the βB850 = 823 nm, and the B800 = 800 nm.

TABLE 4: Relaxation Constants Used in Cases I and II[a]

	relaxation constants $\hbar\gamma$ (cm^{-1})	
sites	case I	case II
αB850	110	2.2
βB850	110	2.2
B800	110	2.7
$(\alpha B850-\beta B850)_1$	12.1	4.4
$(\alpha B850-\beta B850)_2$	11.0	4.2
B800−αB850	1.3	19.8
B800−βB850	1.1	16.5
B800−B800	1.3	19.8

[a] $\bar{\gamma} = \gamma$.

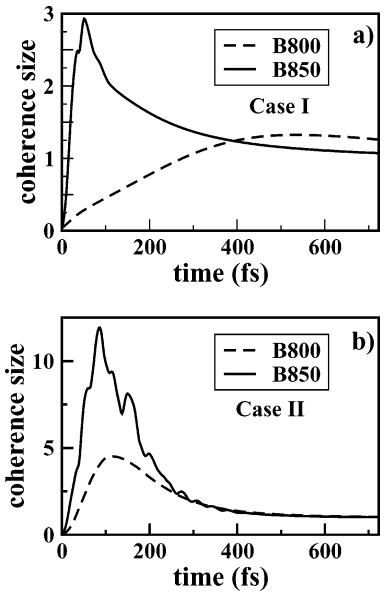

Figure 8. Exciton dynamics in the B800−B850 composite system for two different sets of relaxation constants (Table 4). In case I, placing the initial excitation on the B800 chromophore results in no build-up of coherence. In case II, there is coherence build-up when either the B800 or B850 chromophore is initially excited.

systems. If the effects are significant, this would influence the design of synthetic systems, and be relevant to experiments related to optimal energy transfer. In this section, a composite B800−B850 assembly is studied using the coupling parameters in Table 3.[7a,b] Although all of the couplings were considered, only the largest are given in the table. The interaction between the B800 chromophores and the B850−B800 chromophores is of the same order of magnitude, whereas the B850−B850 coupling is much larger. There are two issues which govern exciton dynamics within the composite system: the rate of transfer of population between the two chains of chromophores and the rate of decay of coherences within the B850 ring. The temporal evolution of excitation initially localized in the B800 ring is found to be very different from the case where initial excitation is localized in the B850 ring. The exciton migration

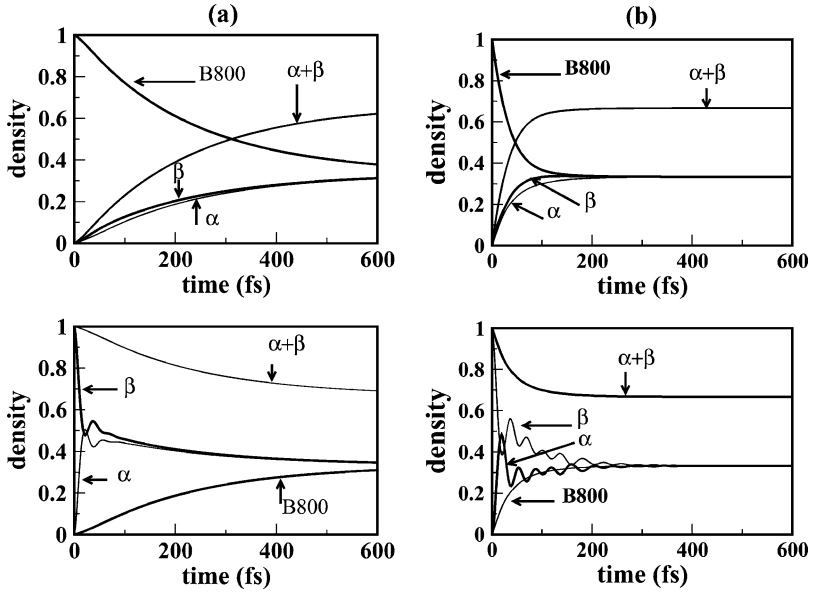

Figure 9. Population densities plotted as a function of time for (a) case I and (b) case II parameters. In (a), the population transfer from B800−B850 when the B800 chromophore is excited is slow compared to the transfer from B850−B850 when the B850 chromophore is excited. In (b), the population transfer rates from B800−B850 are comparable to the B850−B850 transfer rate when either the B800 and B850 chromophores are excited.

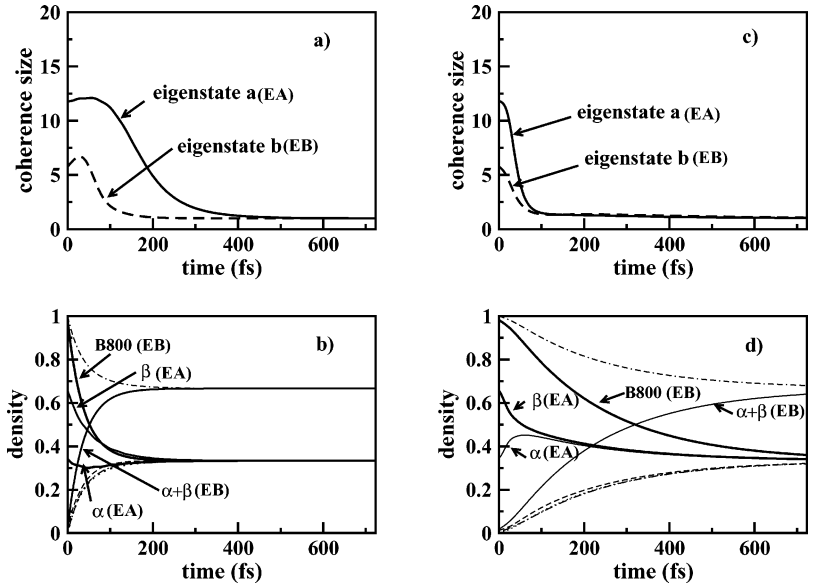

Figure 10. Temporal evolution of coherence and population densities when eigenstates **EA** and **EA** (described in the text) are excited using case I parameters in (a) and (b) and case II paramters in (c) and (d).

is studied here using two very different sets of relaxation parameters to highlight the competition and interplay between population transfer rates and the rate of decay of coherences. In case I, the relaxation constants are based on estimates of the homogeneous line width of the exciton absorption bands (Table 4). In case II, the relaxation constants are adjusted so as to artificially enhance transfer rates between the B800 and the B850 rings. As shown in Figure 8a, excitation of the B800 chromophore leads to practically no build up of coherence in the composite system using the experimentally based relaxation parameters of case I. However, excitation of the B850 chromophore with the same set of parameters leads to significant build up of coherence. For case II, shown in Figure 8b, coherence build up occurs in both cases, though it is larger when the B850 ring is directly excited. A plot of the population transfer from the excited chromophore to the other chromophores in Figure 9a shows the transfer rate from B800 to B850 is slow and the B850−B850 transfer rates are fast in case I. When the transfer to the ring is artificially enhanced, as in Figure 9b, the B800−B850 and B850−B850 transfer rates are comparable and the coherence size is not as dependent on the site of initial excitation.

This behavior can be understood by exciting two eigenstates, one with mainly B800 character **EA** and another with mainly B850 character **EB**, using the relaxation parameters in cases I and II. As shown in Figure 10, parts a and b, for case I, the population transfer rate from the B800 to the B850 chromophores is much slower than the coherence decay rate. In case II (Figure 10, parts c and d), population transfer rates and coherence decay occur on similar time scales. The absence of coherence build up when the B800 chromophore is excited in case I (a model of the real LH2 subunit) is due to slow transfer of excitation to the eigenstates of the B850 chromophore as compared to coherence decay within the B850 ring system. In

the artificial system, when the population transfer rate between the B800 and B850 chromophores matches or exceeds the coherence decay rate within the B850 ring, a build up of coherence is observed in the B850 system. Based on these results, it is conjectured that an experimental study of exciton migration within the B850 ring upon direct excitation of the B850 chromophores should yield different coherences in the ring than the case where the B800 chromophore is initially excited and energy transferred to the B850 ring.

V. Conclusions

The processes involved in converting solar energy to useful electrochemical energy in photosynthesis have been the subject of several experimental and theoretical studies.[4] Photosynthetic light harvesting units that are found in nature are extremely efficient. Reconstitution of light-harvesting systems found in bacteria have produced biomimetic hybrid biological−chemical structures that contain units held together by a protein environment.[3] The relevant time scales involved in transferring energy between antenna complexes and from the light harvesting complexes to the reaction center in the photosynthetic process are known fairly accurately.[4b,14−16] The crystal structure of LH2 has provided the orientations and exact separations between the BCHL units of this light harvesting assembly.[5,6] Using this structural information, effective Hamiltonians for these light-harvesting systems have been proposed and tested against experiments. Although electronic structure calculations are used to generate the excitonic matrix elements, the coupling of this Hamiltonian to the fluctuations of the protein and solvent environment cannot be calculated from first-principles approaches. Because of this, a number of models have tried to address the question of whether excitation transfer occurs coherently or as a result of incoherent hopping within an antenna assembly. These calculations have employed the Forster formalism, stochastic master equations and even the Redfield equations to determine the mechanism of energy transport.[14,26,32] Although some uncertainty in the interaction Hamiltonian between the system and bath still exists, comparison with experiments of LH2 complexes suggests that the hopping mechanism is not correct. Estimates of the coherence length within the LH2 assembly range between two and five sites.[9,14,20,23]

The understanding of the mechanism of energy transfer in antenna systems has grown steadily over the past few years. With the design of synthetic mimics and analogues, the question as to how assemblies can be optimized for energy transfer and what can be learned from the assemblies in nature has become very important. The Haken−Strobl parametrization[31] of the stochastic Liouville equation has been used here to model the energy transfer properties of model light-harvesting systems. This approach is useful insofar as it leads to a large reduction in the computational effort when studying energy transfer in symmetric systems. In addition, the formulation is elegant and conceptually simple. A limitation of this method is that the long-time dynamics asymptotes to the infinite temperature limit and consequently this work has therefore focused on the properties of the short-time dynamics.

In this study, excitation energy transfer in various model light harvesting systems is examined in order to understand how their behavior depends on the geometric arrangement of the monomers. By using monomeric systems taken from the LH2 found in nature, comparisons of various arrangements can be made using the same system and dissipative bath parameters. Our studies have examined the role of monomer arrangements in simple B850 18-membered rings. We have shown that exciton dynamics is fairly insensitive to a reasonable variation in the system parameters such as dimerization and coupling strength. Dimerization and differences in site energies in the B850 ring have little impact on energy transfer within the ring, although they could have a greater impact on energy transfer within the composite B800−B850 system, because this could alter the energy gap between the two rings. Bath induced fluctuations, like the site energy fluctuations and fluctuations in the coupling strengths, are shown to change the coherence size quite dramatically. Previous studies using the Redfield equations to model energy transfer in composite B800−B850 systems also find that the dynamics is fairly sensitive to the bath relaxation parameters.[26] Comparison with these studies has shown that the parametrized stochastic Liouville equation gives the right excitation energy transfer behavior and that the system parametrization chosen in this study is reasonable.

The effect of ring size on energy transfer within B850 ring systems has also been done using the SLE. We have found that the coherence size increases with ring size initially and saturates at higher ring sizes when varied from 4 to 18 monomers. The trend is mirrored closely by changes in the next-to-nearest neighbor couplings within the rings. A comparison was also made with linear chains with the same number of chromophores as the corresponding rings. One of the most interesting results of this work is that it is found that the coherence sizes are much smaller for linear arrangements of the same components. There is also no saturation in coherence size with increasing numbers of dimers in the linear chains. From this, it can be concluded that the presence of the circular symmetry stabilizes the light harvesting array with respect to dynamic disorder. Several of the light harvesting assemblies found in nature display circular symmetry.

Whereas the initial calculations focused on the characteristics of energy transfer in an isolated B850 aggregate, in nature, the structure of light-harvesting assemblies is much more complex. To funnel light energy to be converted to a useful form, efficient light harvesting arrays need to have many coupled arrays arranged as part of a much larger assembly. Consequently, we have also studied energy transfer characteristics of composite ring systems. In particular, we have looked at coupled B800−B850 rings, like those found in LH2. We have shown that the initial mode of excitation has a significant impact on the excitation transfer dynamics. When the B800 chromophore is initially excited, there is a very small build up of coherence in the B850 ring system, whereas localization of the initial excitation on the B850 chromophore leads to much higher coherence sizes. This effect arises due to the interplay between energy transfer rates between the B800 and B850 ring and the coherence decay rates within the B850 ring system.

The results of this present study highlight the effects of different geometries and circular boundary conditions on energy transfer and coherence size in model antenna systems. Most importantly, it is found that circular arrays have larger coherence sizes than other geometries. This is an interesting result that warrants further study. Because the SLE is not an exact solution of the many-body problem, other approximate methods, like the Redfield formalism, will be applied to model systems with significant static disorder that will be compared with the present work.[44,45] In addition, the modeling of extensive assemblies consisting of many antenna arrays will be required to keep pace with experimental progress. Further work will also focus on studying the effects of tailored pulses on the optimization of energy transfer in light-harvesting systems of different geometries.

Acknowledgment. This work is supported by the NSF (Grant No. 9875230) and the Petroleum Research Fund administered by the American Chemical Society. D.G.E. is a Cottrell Scholar of the Research Corporation and a Camille Dreyfus Teacher-Scholar.

References and Notes

(1) Holten, D.; Bocian, D. F.; Lindsey, J. S. *Acc. Chem. Res.* **2002**, *35*, 57.

(2) (a) Kodis, G.; Liddell, P. A.; de la Garza, L.; Clausen, P. C.; Lindsey, J. S.; Moore, A. L.; Moore, T. A.; Gust, D. *J. Phys. Chem A* **1999**, *106*, 2036. (b) Andronov, A.; Gilat, S. L.; Frechet, J. M. J.; Ohta, K.; Neuwahl, F. V. R.; Fleming, G. R. *J. Am. Chem. Soc.* **2000**, *122*, 1175. (c) Kopelman, R.; Shortreed, M.; Shi, Z. Y.; Tan, W. H.; Xu, Z. F.; Moore, J. S.; BarHaim, A.; Klafter, J. *Phys. Rev. Lett.* **1997**, *78*, 1239.

(3) Wolf-Klein, H.; Kohl, C.; Mullen, K.; Paulsen, H. *Angew. Chem.-Int. Ed.* **2002**, *41*, 3378.

(4) (a) Schulten, K. In Simplicity and Complexity in Proteins and Nucleic acids. From simplicity to complexity and back; Frauenfelder, H., Deisenhofer, J., Wolynes, P. G., Eds.; Dahlem University Press: Berlin, 1999; pp 227. (b) Sundstrom, V.; Pullerits, T.; van Grondelle, R. *J. Phys. Chem. B* **1999**, *103*, 2327. (c) Novoderezhkin, V.; Monshouwer, R.; van Grondelle, R. *J. Phys. Chem. B* **1999**, *103*, 10540. (d) Renger, T.; May, V.; Kuhn, O. *Phys. Rep.* **2001**, *343*, 137.

(5) McDermott, G.; Prince, S. M.; Freer, A. A.; Hawthornewaite-Lawless, A. M.; Papiz, M. Z.; Cogdell, R. J.; Isaacs, N. W. *Nature (London)* **1995**, *374*, 517.

(6) Koepke, J.; Hu, X.; Muenke, C.; Schulten, K.; Michel, H. *Structure* **1996**, *4*, 581.

(7) (a) Krueger, B. P.; Scholes, G. D.; Fleming, G. R. *J. Phys. Chem. B* **1998**, *102*, 5378. (b) Scholes, G. D.; Gould, I. R.; Cogdell, R. J.; Fleming, G. R. *J. Phys. Chem. B* **1999**, *103*, 2543. (c) Alden, R. G.; Johnson, E.; Nagarajan, V.; Parson, W. W.; Law, C. J.; Cogdell, R. J. *J. Phys. Chem. B* **1997**, *101*, 4667. (d) Sauer, K.; Cogdell, R. J.; Prince, S. M.; Freer, A. A.; Isaacs, N. W.; Scheer, H. *Photochem. Photobiol.* **1996**, *64*, 564.

(8) Xiche, H.; Ritz, R.; Damjanovic, A.; Schulten, K. *J. Phys. Chem. B* **1997**, *101*, 3854.

(9) Damjanovic, A.; Kosztin, I.; Kleinekathofer, U.; Schulten, K. *Phys. Rev. E* **2002**, *65*, 031919−1.

(10) (a)Wu, H.-M.; Savikhin, S.; Reddy, N. R. S.; Jankowiak, R.; Cogdell, R. J.; Struve, W. S.; Small, G. J. *J. Phys. Chem.* **1996**, *100*, 12022.

(11) Ritz, T.; Park, S.; Schulten, K. *J. Phys. Chem. B* **2001**, *105*, 8259.

(12) Herek, J. L.; Fraser, N. J.; Pullerits, T.; Martinsson, P.; Polivka, T.; Scheer, H.; Cogdell, R. J.; Sundstrom, V. *Biophys. J.* **2000**, *78*, 2590.

(13) van der Laan, H.; Schimdt, Th.; Visschers, R. W.; Visschers, K. J.; van Grondelle, R.; Volker, S. *Chem. Phys. Lett.* **1990**, *170*, 231. Hess, S.; Visschers, K. J.; Pullerits, T.; Sundstrom, V.; Hunter, C. N. *Biochemistry* **1994**, *33*, 8300.

(14) Jimenez, R.; Dikshit, S. N.; Bradforth, S. E.; Fleming, G. R. *J. Phys. Chem.* **1996**, *100*, 6825.

(15) Shreve, A. P.; Trautman, J. K.; Frank, H. A.; Owens, T. G.; Albrecht, A. C. *Biochim. Biophys. Acta* **1991**, *1058*, 280. Hess, S.; Feldchtein, F.; Babin, A.; Nurgaleev, I.; Pullerits, T.; Sergeev, A.; Sundstrom, V. *Chem. Phys. Lett.* **1993**, *216*, 247.

(16) Salverda, J. M.; van Mourik, F.; van der Zwan, G.; van Grondelle, R. *J. Phys. Chem. B* **2000**, *104*, 11395. Agarwal, R.; Yang, M.; Xu, Q.-H.; Fleming, G. R. *J. Phys. Chem. B* **2001**, *105*, 1887.

(17) van Grondelle, R.; Novoderezhkin, V. *Biochemistry* **2001**, *40*, 15057.

(18) (a) Koolhaas, M. H. C.; van der Zwan, G.; Freese, R. N.; van Grondelle, R. *J. Phys. Chem. B* **1997**, *101*, 7262. (b) Koolhaas, M. H. C.; van der Zwan, G.; van Grondelle, R. *J. Phys. Chem. B* **2000**, *104*, 4489.

(19) Monshouwer, R.; Abrahamsson, M.; van Mourik, F.; van Grondelle, R. *J. Phys. Chem. B* **1997**, *101*, 7241.

(20) Pullerits, T.; Chachisvilis, M.; Sundstrom, V. *J. Phys. Chem.* **1996**, *100*, 10787.

(21) Chachisvilis, M.; Kuhn, O.; Pullerits, T.; Sundstrom, V. *J. Phys. Chem. B* **1997**, *101*, 7275.

(22) Dahlbom, M.; Pullerits, T.; Mukamel, S.; Sundstrom, V. *J. Phys. Chem. B* **2001**, *105*, 5515.

(23) Ray, J.; Makri, N. *J. Phys. Chem. A* **1999**, *103*, 9417.

(24) (a) van Oijen, A. M.; Ketelaars, M.; Kohler, J.; Aartsma, T. J.; Schmidt, J. *Science* **1999**, *285*, 400. (b) van Oijen, A. M.; Ketelaars, M.; Kohler, J.; Aartsma, T. J.; Schmidt, J. *Biophys. J.* **2000**, *78*, 1570. (c) van Oijen, A. M.; Ketelaars, M.; Kohler, J.; Aartsma, T. J.; Schmidt, J. *J. Phys. Chem. B* **1998**, *102*, 9363.

(25) (a) Redfield, A. G. *Adv. Magn. Reson.* **1965**, *1*, 1. (b) Jean, J. M.; Friesner, R. A.; Fleming, G. R. *J. Chem. Phys.* **1992**, *96*, 5827.

(26) (a) Kuhn, O.; Sundstrom, V. *J. Phys. Chem. B* **1997**, *101*, 3432. (b) Kuhn, O.; Sundstrom, V. *J. Chem. Phys.* **1997**, *107*, 4154.

(27) (a) Shortreed, M. R.; Swallen, S. F.; Shi, Z. Y.; Tan, W. H.; Xu, Z. F.; Devadoss, C.; Moore, J. S.; Kopelman, R. *J. Phys. Chem. B* **1997**, *101*, 6318. (b) Raychaudhuri, S.; Shapir, Y.; Chernyak, V.; Mukamel, S. *Phys. Rev. Lett.* **2000**, *85*, 282.

(28) Matsuzaki, S.; Zazubovich, V.; Fraser, N. J.; Cogdell, R. J.; Small, G. J. *J. Phys. Chem. B* **2001**, *105*, 7049.

(29) Fidder, H.; Knoester, J.; Wiersma, D. A. *J. Chem. Phys.* **1991**, *95*, 7880.

(30) Bakalis, L. D.; Coca, M.; Knoester, J. *J. Chem. Phys.* **1999**, *110*, 2208.

(31) (a) Haken, H.; Strobl, G. *Z. Phys.* **1973**, *262*, 135. (b) Reineker, P. In Springer tracts in modern physics. *Exciton dynamics in molecular crystals and aggregates*; Hohler G., Ed.; Springer, Berlin, 1982; Vol. 94, p 111.

(32) Capek, V.; Szocs, V. *Phys. Stat. Sol. (B)* **1985**, *131*, 667.

(33) Mathematica 4.1 for Linux, Copyright 1988−2000 Wolfram Research, Inc.

(34) Wolfram, S. *The Mathematica Book*, 3rd ed.; Cambridge University Press: New York, 1996.

(35) Meier, T.; Chernyak, V.; Mukamel, S. *J. Phys. Chem. B* **1997**, *101*, 7332.

(36) Liuolia, V.; Valkunas, L.; van Grondelle, R. *J. Phys. Chem. B* **1997**, *101*, 7343.

(37) Szocs, V.; Banacky, P. *Chem. Phys.* **1994**, *186*, 161.

(38) Herman, P.; Barvik, I. *J. Phys. Chem. B* **1999**, *103*, 10892.

(39) Yeow, E. K. L.; Haines, D. J.; Ghiggino, K. P.; Padden-Row, M. N. *J. Phys. Chem. A* **1999**, *103*, 6517.

(40) (a) Jang, S.; Dempster, S. E.; Silbey, R. J. *J. Phys. Chem. B* **2001**, *105*, 6655. (b) Dempster, S.; Jang, S.; Silbey, R. J. *J. Chem. Phys.* **2001**, *114*, 10015.

(41) Koolhaas, M. H. C.; Frese, R. N.; Fowler, G. J. S.; Bibby, T. S.; Georgakopoulou, S.; van der Zwan, G.; Hunter, C. N.; van Grondelle, R. *Biochemistry* **1998**, *37*, 4693.

(42) Herek, J. L.; Wohlleben, W.; Cogdell, R. J.; Zeidler, D.; Motzkus, M. *Nature* **2002**, *417*, 533.

(43) Jimenez, R.; van Mourik, F.; Yu, J. Y.; Fleming, G. R. *J. Phys. Chem. B* **1997**, *101*, 7350.

(44) Yang, M.; Fleming, G. R. *Chem. Phys.* **2002**, *275*, 355.

(45) Kalyanaraman, C.; Evans, D. G. *Chem. Phys. Lett.* **2000**, *324*, 459.